

Model Systems for the Investigation of the Opsin Shift in Bacteriorhodopsin

Lars Lasogga and Wolfgang Rettig*

Institut für Chemie, Humboldt-Universität zu Berlin, 12489 Berlin, Germany

Harald Otto and Ingrid Wallat

Institut für Experimentalphysik, Freie Universität Berlin, 14195 Berlin, Germany

Julia Bricks

Institute of Organic Chemistry NASU, Kiev 02094, Ukraine

Received: May 4, 2009; Revised Manuscript Received: November 16, 2009

Donor–acceptor substituted styrenes and phenylbutadienes with substituents varying in donor and acceptor strength and as reconstituted chromophore–protein complexes were investigated as model compounds for the protonated Schiff base chromophore in bacteriorhodopsin (bR) both experimentally and theoretically. Charge distribution, donor–acceptor strength, and the shift of the absorption energy are correlated. The effect of the external electrostatic field was tested with a compound carrying an additional nonconjugated charge. The concept of overpolarization by the external charge, that is, the reversal of the relative importance of the two main resonance structures in S_0 and S_1 , has been emphasized and related to a simple qualitative 2×2 interaction model. The variable donor approach is a new way for a better understanding of the Opsin shift in Bacteriorhodopsin.

Introduction

One of the most discussed questions in the mechanism of vision is the reason for the bathochromic shift in the spectra of the chromophore: whereas the unbound free chromophore has an absorption maximum near the blue end of the visible spectrum, the absorption maximum is red-shifted for the chromophore bound to the protein via a protonated retinal Schiff base linkage (PRSB). Recently, X-ray structural data^{1–3} have been determined for the visual chromophore Rhodopsin (Rh) and its closely related bacterial variant Bacteriorhodopsin (bR) to a sufficient accuracy such that the role of the different amino acids in the protein backbone and their effect on the absorption spectra could be simulated by quantum chemical models (see, e.g., refs 4 and 5). In spite of that, the relative importance of the different factors determining the Opsin shift, that is, the absorption difference between the chromophore in solution and embedded in the protein, is still a matter of controversy.

These factors which are most discussed for the Opsin shift^{4–6} are (i) the counterion near the Schiff base nitrogen, (ii) the electrostatic field induced by further charged residues or dipolar groups within the protein, (iii) the twisting of the chromophore, and (iv) H-bonding networks.

As investigated previously, factor (i), the counterion influence, seems to be the most important one.^{4,7–9} It is suggested that additional ions such as Na^+ are possibly playing a role.² In this context, factor (ii), the possible negative or positive charges due to protonation of amino end groups in the surrounding protein environment, also has to be taken into account.^{5,9} By contrast, factor (iii), the twisting, plays a less important role in bR as indicated by the nearly planar chromophore found for bR in the X-ray and electron crystallography structure.¹⁰ Also

the H-bond network is of minor importance as concluded in refs 4, 5, and 11.

By following the most important factors (i) and ii), we are lead to an early model, the so-called external point-charge model. It postulates that the wavelength shift is induced by an external charge; that is, charges or dipoles in the surrounding protein are thought to modify the absorption spectrum.^{12–15} Many experimental efforts have been devoted to this question, mostly regarding proteins reconstituted with artificial chromophores related to PRSB. Bridged chromophores were also used to block some of the important photochemical pathways,¹⁶ as well as polar fluorescent probes¹⁷ which can yield information on the electrostatic field within the binding pocket of bR and Rh.

Especially relevant for the interpretation of the Opsin shift is the observation of the absorption energy of PRSB in the gas phase which is red-shifted with respect to that in the protein.¹⁸ This indicates that the role of the negative counterion in the neighborhood of the chromophore is of great importance.

Not only the theoretical understanding of the Opsin shift in bR and in Rh but also the color shift in the visual color cones of Rh which discriminate different parts of the visual spectrum are intricate problems to solve.^{19–22} Here, a further parameter was found to be important. Resonance Raman measurements indicate that for the blue, green, and red pigments, the chromophore vibrations correlate with the absorption energy.^{20,23} A similar correlation is also found when several intermediates of the reaction cycle are compared.²⁴ The electronic absorption energy ΔE_{01} can be correlated with the so-called bond length alternation (BLA),⁹ that is, the deviation from the ideal cyanine behavior where all bonds are of equal length. The correlation between ΔE_{01} and BLA is direct evidence for the change of the electronic distribution induced by the electrostatic field of

* Corresponding author.

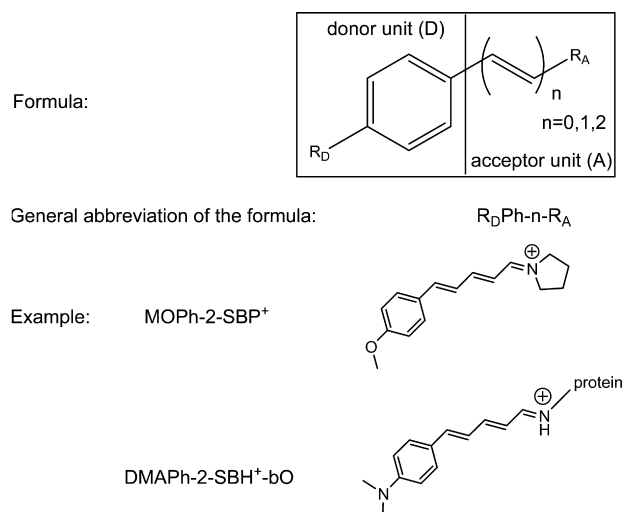


Figure 1. General structure of the investigated compounds with the dissection into donor and acceptor unit. For the abbreviation of the substituents, see Table 1.

the surrounding or of the equivalent effect of donor–acceptor substituents on the chromophore.²⁵

An open point in the relation of X-ray structures and protein-induced fields is the presence of water molecules close to the chromophore.² They can lead to protonation or deprotonation of amino acids in the neighborhood, and the X-ray studies may be subject to some uncertainty regarding the ionization state of the relevant amino acids.

Instead of X-ray-based quantum-chemical calculations, experiments on reconstituted protein complexes can yield a more direct answer of the *in vivo* situation. An early study uses the fluorescence probe PRODAN and compares the results for the protein complex to the spectra of model compounds carrying an additional nonconjugated charge, allowing in principle a direct access to the effective field by comparing the spectral shifts.¹⁷

Related to this study, we use synthetic chromophores here to create reconstituted Bacterioopsin complexes. In addition to the approach of Sheves et al.¹⁷ which uses model compounds with external charges, we also change the donor–acceptor properties of the chromophores. Comparison to solution spectra and to quantum chemical calculations allows us to understand the observed shifts on the basis of electrostatic fields induced by the surrounding and by the donor–acceptor substituents. The quantum-chemical results enable the analysis of the charge distribution and indicate that some of the observed spectral shifts are connected with a reversal of the original charge distribution, explainable with the exchange of the leading resonance structures in the ground and excited states.

Experimental Part

A series of donor–acceptor polyenes were synthesized, with increasing donor strength and some variation of the acceptor (Figure 1, Table 1). Our study focuses on model chromophores for protonated Schiff bases with two double bonds in the chain ($n = 2$). The experimental results are contrasted to quantum-chemical studies which yield the distribution of the positive charge along the backbone of the chromophores.

A model compound with an additional nonconjugated external positive charge was also investigated experimentally in order to analyze more directly the point charge effect, both in an experimental and a theoretical way.

TABLE 1: General Structures and Abbreviations of the Donor and Acceptor Groups of the Model Chromophores^a

donor unit end group R_D		acceptor unit end group R_A	
- H	(H)	- CHO	(CHO)
- CH ₃	(M)		(SBP ⁺)
- HO	(HO)		(SBPip ⁺)
- OCH ₃	(MO)		(SBPip ⁺⁺)
- N(CH ₃) ₂	(DMA)		(SBH ⁺ -bO)

^a For our study, the compound series $n = 2$ was investigated experimentally (see Table 2a parts 1 and 2).

TABLE 2A: List of Compounds Investigated Both Experimentally and Theoretically

1. Compounds to Investigate the Influence of Protein Matrix		
HPh-2-CHO	HPh-2-SBP ⁺	HPh-2-SBH ⁺ -bO
MPh-2-CHO	MPh-2-SBP ⁺	MPh-2-SBH ⁺ -bO
HOPh-2-CHO	HOPh-2-SBP ⁺	HOPh-2-SBH ⁺ -bO
MOPh-2-CHO	MOPh-2-SBP ⁺	MOPh-2-SBH ⁺ -bO
DMAPh-2-CHO	DMAPh-2-SBP ⁺	DMAPh-2-SBH ⁺ -bO
2. Compounds to Investigate the Influence of an Additional Nonconjugated External Charge		
MOPh-1-SBP ⁺	MOPh-1-SBPip ⁺	MOPh-1-SBPip ⁺²

TABLE 2B: List of Additional Compounds Investigated Theoretically

1. Compounds of the $n = 2$ Series with Respect to Table 2a Part 1		
HPh-2-SBPip ⁺	HPh-2-SBPip ⁺²	
MPh-2-SBPip ⁺	MPh-2-SBPip ⁺²	
HOPh-2-SBPip ⁺	HOPh-2-SBPip ⁺²	
MOPh-2-SBPip ⁺	MOPh-2-SBPip ⁺²	
DMAPh-2-SBPip ⁺	DMAPh-2-SBPip ⁺²	
2. Compounds of the $n = 1$ Series with Respect to Table 2a Part 2		
HPh-1-SBP ⁺	HPh-1-SBPip ⁺	HPh-1-SBPip ⁺²
MPh-1-SBP ⁺	MPh-1-SBPip ⁺	MPh-1-SBPip ⁺²
HOPh-1-SBP ⁺	HOPh-1-SBPip ⁺	HOPh-1-SBPip ⁺²
DMAPh-1-SBP ⁺	DMAPh-1-SBPip ⁺	DMAPh-1-SBPip ⁺²

Synthesis

The aldehydes listed in Table 2a were synthesized according to the general approach described in ref 26.

In some cases, protecting groups had to be used as described in detail in ref 27. The corresponding SBP⁺ salts were prepared by reacting the substituted aldehydes with pyrrolidine perchlorate in isopropanol.

SBPip⁺ compounds were prepared by reaction of substituted aldehydes with commercially available 1-Boc-piperazine (tert-butyl piperazine-1-carboxylate) followed by cleavage of the resulting Boc-protected SBPip⁺ compounds with trifluoroacetic acid yielding the corresponding SBPip⁺² derivatives.

All compounds were purified by column chromatography and/or recrystallized before use, and their structure was confirmed by NMR. The synthetic details are described in ref 27.

Spectroscopy

For experimental solution spectra, we used ethanol, DMSO, THF, and acetonitrile from Merck (Uvasol grade). Absorption spectra were measured on a Unicam UV4 spectrometer.

The SBP^+ compounds are not stable in solution and convert to the aldehyde. To get more information on this effect, we investigated the SBP^+ compounds by time-resolved absorption measurements in two solvents (DMSO and THF). The conversion times turned out to be in the order of many hours, whereas the measurement of spectra took less than 10 min, during which the conversion changes can be neglected. The time when half the conversion had occurred was about 5 h in the fastest case.

The fit of the absorption spectra which were corrected for the solvent background was done by a PeakFit auto fit routine with a log-normal-4 function.²⁸ For the protein-reconstitution experiments, Bacterioopsin was harvested from halobacterial strain JW5 (the retinal deficient mutant) in water²⁹ and regenerated at room temperature in the dark with the model chromophores dissolved in ethanol. The reconstitution spectra were measured on a Shimadzu UVPC 2102 spectrometer. The reproducibility of the spectra was tested and was satisfactory.

The absorption spectra of the chromophore–protein complexes were evaluated in the following way. The spectra at $t_0 = 0$ were subtracted from the measured spectra at later times, and the resulting (negative) signals of the time-dependent difference spectra clearly showed the increasing signal of the chromophore bound to the protein and the decreasing signal of the corresponding unbound aldehydes. Fitting was done with the log-normal-4 function. For detail, see Figure S1 in the Supporting Information.

It can be deduced from a competition experiment with the model chromophore $MOPh-2-CHO$ that the binding to the protein occurs at the binding site of the native chromophore, and we assume that this also holds for the other model compounds. For the competition experiment, the chromophore $MOPh-2-CHO$ was added to the protein in the ratio 1:1. After the regeneration of the chromophore–protein complex, the native retinal was added in the ratio 1:1. Therefore, it could be observed that the model chromophore was replaced by the native retinal as deduced from the appearance of the spectra of bR (see Figure S2 in the Supporting Information).

The reconstitution kinetics were measured for about 72 h.

Calculations

For the quantum-chemical calculations, the GAUSSIAN 03 package was used.³⁰ At first, the molecular structure was optimized in the ground state by using the AM1 method and the DFT method. Three sets of calculations were done: (a) the entire molecule, (b) the donor moiety (D) with the acceptor unit substituted by H, and (c) the corresponding acceptor moiety (A) with the donor unit substituted by H (see Figure 1). From the donor moiety (b) and the acceptor moiety (c), the energies of the frontier orbitals HOMO(D) and LUMO(A) were taken. The difference of these two energies was defined as the donor–acceptor strength ΔE_{DA} of the entire molecule, $\Delta E_{DA} = E_{HOMO(D)} - E_{LUMO(A)}$. The so defined ΔE_{DA} is a theoretically derived value to measure the strength of a donor–acceptor complex. It is equivalent to the difference of ionization potential and electron affinity of the moieties.

The optimized structures from (a) were taken to calculate the Franck–Condon transition energies by using the ZINDO/S method and the TDDFT method embedded in GAUSSIAN 03.

Results

The absorption spectra of the uncomplexed aldehydes, of the SBP^+ model compounds, and of the protein complexes, after the PeakFit analysis, are displayed in Figure 2, and their absorption maxima are given in Table 3. A red shift is observed

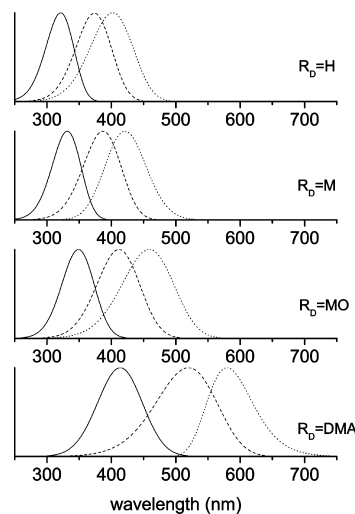
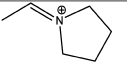
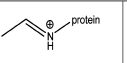


Figure 2. Comparison of the longest-wavelength absorption bands of the chromophores $R_D-Ph-2-R_A$ with the aldehyde ($R_A = CHO$, solid line) and the SBP^+ ($R_A = SBP^+$, dashed line) model compounds and spectra of the reconstituted Bacterioopsin-dye complexes ($R_A = SBH^+-bO$, dotted line) recovered from a PeakFit analysis for various donor and acceptor end groups R_D and R_A . The experiments were done in EtOH for the CHO and SBP^+ compounds and in water for bO. In the latter case, EtOH is only present in a very small amount.

TABLE 3: Experimental Absorption Maxima of the $n = 2$ Series with Neutral and Charged Acceptor Groups R_A and Donors R_D of Increasing Strength and Acceptor End Groups in Solution and in Protein Matrix^c

donor end group R_D	acceptor end group R_A			opsin shift ^{a)} [10^3 cm^{-1}]	
					
	(CHO)	(SBP^+)	(SBH^+-bO)		
absorption maxima nm					
		[EtOH]	[EtOH]	[Water] ^{b)}	
- H (H)	323	378	406	1820	
- CH ₃ (M)	334	391	423	1930	
- OH (HO)	357	433	480	2260	
- OCH ₃ (MO)	351	420	459	2020	
- N(CH ₃) ₂ (DMA)	416	533	580	1520	

^{a)} The Opsin shift is the difference of absorption wavenumbers of the SBP^+ compound in solution and of the SBH^+-bO complex.

^{b)} With maximal 0.5% EtOH, see spectroscopy part. ^{c)} For some donors, the protonated *n*-butyl complexes were also synthesized. The experimental spectra do not differ significantly. Furthermore, calculations of spectra with the GAUSSIAN 03 ZINDO/S routine give the same result for both *n*-butyl complexes and SBP^+ compounds.

when either donor or acceptor strength are increased. In every case, the spectra of the Bacterioopsin complexes are most red-shifted. On the basis of the red shift of the model compounds in solution, these spectra of the Bacterioopsin complexes indicate that the chromophore in the protein behaves as if the donor and the acceptor are stronger than in the corresponding SBP^+ derivatives in solution.

Figure 3 shows that the calculated absorption energies of the chromophores correlate approximately linearly with the calculated fraction of positive charge located on the donor groups of increasing strength. In solution, polarizability effects are active, increase Q_D , and reduce the absorption energy because the counterion and/or the polar solvent will tend to shift the positive charge toward the acceptor end, quite similar to the effect of increasing donor strength of the model compounds used here. This leads to an increase of Q_D and to a red shift for the

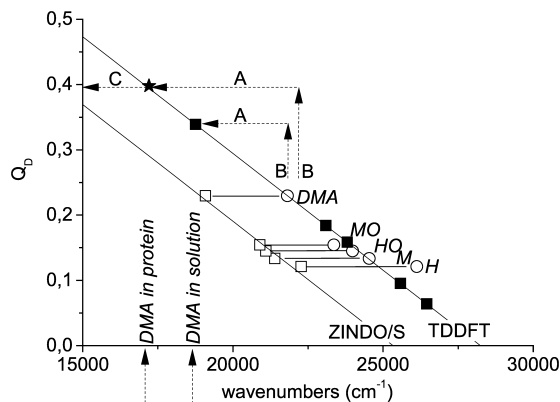


Figure 3. Fraction of the positive charge Q_D (for the optimized ground-state geometry) located on the donor unit of the SBP^+ compounds (as defined in Figure 1) plotted versus the absorption energy. The calculated gas-phase absorption shifts to the red, and the charge localized on the donor (Q_D is given in units of the elementary charge) increases as a function of the donor strength (approximately linear correlation as shown). Strong polarization effects especially for the DMA donor lead to a red shift of the gas-phase absorption (\circ for TDDFT [b3lyp/6-31G**]) for the solution surrounding (\blacksquare , in Ethanol solvent) and the protein surrounding (\blackstar). This red shift is indicated by arrows A. The corresponding increase of Q_D (charge shift toward the donor D) due to the surrounding is indicated by arrows B. The experimental absorption of the chromophore–Bacterioopsin complex yields an approximate value for the effective charge distribution Q_D of the DMA model chromophore inside the protein (arrow C). The effective Q_D values are collected in Table 4.

experimental points with respect to the calculated ones. This effect is larger for the DMA compound than for the H compound because of the larger electronic polarizability. In fact, the nearly identical calculated and measured absorption energies for the H to the MO donors yield an identical correlation line and indicate that polarizability effects are weak in this case. The extrapolation of the correlation line to the DMA compound together with the experimental absorption energy allows us to determine the effective Q_D in solution including polarizability effects (Table 4; see also caption of Figure 3).

The donor and acceptor strength and their combined influence can be quantified by the parameter ΔE_{DA} . The latter is derived from the HOMO and LUMO energies of the donor and acceptor units (Figure 1, Table 4) as described in the Experimental Part. Figure 4 reveals that the absorption energies correlate with the donor–acceptor strength ΔE_{DA} . As discussed below (see eq 4), the correlation is expected to follow a parabola, but because of the small range in the experimental case, it can be approximated by a linear fit.

The SBP^+ derivatives (Figure 1) are a good model for the chromophore in the Bacterioopsin complex as long as the protein surrounding is not considered. Consequently, both chromophores differ little in ΔE_{DA} values in vacuum, but anisotropic medium effects such as the protein can change this value. The additional red shift for the Bacterioopsin complex as compared to ethanol solution is therefore due to medium-difference effects: ethanol versus protein matrix. This medium influence—as discussed in Figure 8—can be determined quantitatively. From the experimental absorption maximum of the Bacterioopsin complexes, the protein-induced change of ΔE_{DA} can be determined from the correlation yielding an effective ΔE_{DA} for the protonated Schiff base chromophore embedded in the protein. For example, for $R_D = \text{DMA}$, ΔE_{DA} shifts from $\Delta E_{DA} \approx -2.7$ eV for the SBP^+ derivative to $\Delta E_{DA} \approx -0.7$ eV for the Bacterioopsin complex corresponding to an effectively increased donor–acceptor strength, induced by the protein matrix. A similar extrapolation

can be done for Q_D from Figure 3, and the values are included in Table 4. The increased ΔE_{DA} for the protein complex leads to a significant increase of the charge on the donor unit.

Discussion

A. Correlation of Chemical Structure, Absorption Maxima, and Chromophore Charge Distribution. Consequences of the Polymethine Model. The absorption maxima of the chromophores in the Bacterioopsin complexes are red-shifted with respect to the solution spectra of the ionic model compounds (acceptor = SBP^+) in all cases. This shows that, for example, the effective donor strength in the protein complex $DMAPh-2-SBP^+ - bO$ is considerably larger than that for $DMAPh-2-SBP^+$ in polar solution. The apparently larger donor strength cannot be due to bulk polarity effects of the surrounding medium, because ionic compounds such as $DMAPh-2-SBP^+$ with two nitrogens at either end show little solvatochromy, similar to closely related other ionic donor–acceptor compounds.³¹

A vectorial electrostatic field can, however, be induced by the protein surrounding, yielding spectral shifts also for these ionic compounds, similar to those for the neutral dipolar compounds, as long as the charge distribution is different for the S_0 and S_1 states. In our case, the protein spectra are all red-shifted with respect to the solution spectra indicating that the S_1 is more stabilized by the field than the S_0 state.

Alternatively, the red-shifted absorption spectra can be described by the so-called polymethine or cyanine model which predicts that the most symmetric electronic structure and charge distribution lead to the lowest absorption energy for linear cyanines and that asymmetric charge distributions lead to blue-shifted spectra.³²

The basic mechanism responsible for the cyanine model can be found in the interaction of the two possible resonance structures for symmetric as well as asymmetric cyanines, as for example discussed in refs 33–37. The absorption is of lowest energy when the contribution of the two resonance structures is equal (so-called cyanine limit, CL). For our case, an example for the two resonance structures is given in Figure 5.

A significant change of the relative weight of the two possible resonance structures can be induced either by changing the donor and/or acceptor strength or by the influence of external charges. In early work, the strongly red-shifted absorption spectra of the proteins (Rh or bR) have been explained within this external-charge model by negative charges placed along the retinal Schiff base chain, far away from the Schiff base nitrogen, with an additional negative charge due to the counterion near the Schiff base end.^{4,12,13} In our charge-shift-model compounds, donors shift better the positive charge away from the Schiff base nitrogen and shift the spectra to the red (Figure 3). This corresponds to a more symmetric charge distribution. A similar charge shift and accompanying absorption red shift would be induced by placing a positive charge in the neighborhood of the end of the chromophore with surplus positive charge (Schiff base nitrogen) or by placing a negative charge near the opposite end as assumed in the external-charge model. In both cases, the consequence will be a more symmetric charge distribution, closer to that of symmetric cyanines, and the absorption will therefore shift to the red.³² The opposite effect will result from a negative charge near the Schiff base nitrogen or a positive one at the other end.

By applying this point of view to the observed absorption data of protonated retinal Schiff base in vacuum (610 nm)³⁸ and methanol solution (440 nm)³⁹ as well as in bR (570 nm),⁴⁰ we can interpret the strong blue shift from vacuum to the

TABLE 4: Summary of the Calculated Donor–Acceptor Strength ΔE_{DA} (Derived from the HOMO Energy of the Donor Moiety (D) and the LUMO Energy of the Acceptor Moiety (A)) and Transition Energy ΔE_{01}^a

molecule	$E_{\text{HOMO(D)}}^b$	$E_{\text{LUMO(A)}}^b$	ΔE_{DA}^c	$\Delta E_{01}^{\text{calc } d}$	$\Delta E_{01}^{\text{exp } e}$	Q_D^f	ΔE_{DA}^g
HPh–2-SBP ⁺	−9.653	−5.560	−4.093	3.239	3.280	13	−3.952
MPh–2-SBP ⁺	−9.330	−5.560	−3.770	3.043	3.171	16	−3.516
HOPh–2-SBP ⁺	−9.114	−5.560	−3.554	2.974	2.863	26	−2.281
MOPh–2-SBP ⁺	−9.004	−5.560	−3.444	2.896	2.952	23	−2.700
DMAPh–2-SBP ⁺	−8.274	−5.560	−2.714	2.705	2.130	39	−0.701

^a All values are given in eV. As can be seen, an increasing (less negative) ΔE_{DA} leads to a decreasing transition energy. ^b Calculated by GAUSSIAN 03. ^c Calculated difference $E_{\text{HOMO(D)}} - E_{\text{LUMO(A)}}$. ^d Calculated excitation energy by TDDFT (b3lyp/6-31G**). ^e Experimental excitation energy in EtOH. ^f Fraction of positive charge on the donor unit for the corresponding bO complex with respect to the polarization effects, derived from a linear fit of Figure 3 (in percent). ^g Donor–acceptor strength ΔE_{DA} for the bacterioopsin protein complex with respect to the polarization effects, derived from Figure 4.

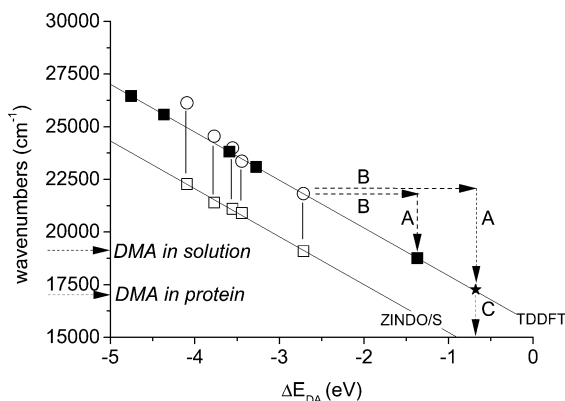


Figure 4. The calculated donor–acceptor strength ΔE_{DA} plotted versus the calculated (\square) and experimental (\blacksquare) absorption maxima of the $n = 2$ SBP⁺ compounds. Experiments are done in EtOH solvent. Polarization effects are analogous to those in Figure 3. The red shift is indicated by arrows A. Polarization also leads to a shift of the donor–acceptor strength indicated by arrow B. The experimental absorption of the chromophore–Bacterioopsin complex yields an approximate value for the effective donor–acceptor strength of the DMA model chromophore inside the protein (arrow C). For the protein data points, it was assumed that the theoretical correlation line is applicable for deriving the effective ΔE_{DA} valid for the protein surrounding (see text). The ΔE_{DA} values are collected in Table 4.

solution spectrum as introduced by the negative counterion located near the positively charged Schiff base end. In the protein, there is a similar counterion close to the Schiff base end. Additional charges in the protein complex can induce the red shift with respect to the solution spectrum according to the external-charge model,^{4,12,13} fully consistent with our qualitative model (see discussion in Figure 8).

The same applies to the compounds like DMAPh–2-SBP⁺ measured here. There will be a counterion in both solution and in the protein, but the protein around the DMAPh–2-SBP⁺–bO complex may create an additional anisotropic electric field leading to a more symmetric charge distribution than in solution and yielding a possible explanation for the observed absorption red shift as compared to the solution spectra.

What is new in our study compared to the previous external-charge studies^{12–14} is that we apply a variation of the donor strength, and the external-charge influence on the charge distribution induced by the same external field can be different (see below Section B).

As mentioned, Förster’s resonance model³⁴ which was later refined by Platt³⁵ as well as the cyanine model of Dähne^{32,36,37} predict that the absorption energy of a simple unsymmetric cyanine is lowest for an approximately evenly distributed positive charge and for resonance structures A and B in Figure 5 of similar energy (compound 1). This situation is called the

CL. The similar energies for resonance structures A and B implies that their weight in the wave function (AB of the molecular system with resonance between the two structures A and B) is 50%. This can be expressed by the condition $c^2 = 0.5$ for the CL in eqs 1 and 2. For unsymmetric cases (compound 2), the contribution of the resonance structures becomes unequal, and the $S_0 - S_1$ energy difference increases, Figure 6.

$$\psi_{AB}(S_0) = c\psi_A + (1 - c^2)^{0.5}\psi_B \quad (1)$$

$$\psi_{AB}(S_1) = (1 - c^2)^{0.5}\psi_A - c\psi_B \quad (2)$$

For the general case, the value of the transition energy ΔE_{01} can be obtained by solving the 2×2 secular determinant (eq 3) involving the interaction energy F as off-diagonal element and the energy difference $b = b_A - b_B$ of the resonance structures,³⁴ resulting in eq 4. This energy difference b is equal to the donor–acceptor strength ΔE_{DA} of the molecule as defined in the calculation section above; therefore, we can write $b = \Delta E_{DA}$. The consequences of this model can be visualized for different values of F and b (Figure 7).

$$\begin{vmatrix} E - b_A & 0.5F \\ 0.5F & E - b_B \end{vmatrix} = 0 \quad (3)$$

$$\Delta E_{01} = \sqrt{F^2 + b^2} \quad (4)$$

Equation 4 allows to predict that for $F \gg b$, the effect on ΔE_{01} by a change of b (corresponding to the variation of substituents DMA to H) will be very small. The contrary is observed (Figure 3), and we can conclude that F is small and the effect of b prevails. Quantitative determination of b and F is however not possible within the accuracy of our data (see Figure 4).

This model predicts that for linear ideal cyanines like structure 1 (Figure 5), the absorption energy becomes 0 (infinite absorption wavelength) for $F = 0$ but cannot become 0 for F of finite size. This is relevant for the prediction of the absorption energy (wavelength) for n toward infinity, for example, in conjugated polymers. Simple cyanine models predict an infinite absorption wavelength for this condition,^{41,42} whereas experimentally, the absorption energy converges to a finite nonzero value,⁴³ which moreover depends on the nature of the end groups, and this is correctly described by the above equations for $F \neq 0$ even for n tending toward infinity and by other more refined models.^{44,45}

The absorption shifts with increasing donor–acceptor difference can be understood on the basis of changes in b if the coupling F of the two main resonance structures is kept constant starting from the CL ($b = 0$, $c^2 = 0.5$). The spectra will blue-shift in both directions of increasing $|b|$, with $b > 0$ being the normal region (structure A more stable) and $b < 0$ being the region where structure B is more stable than structure A (we

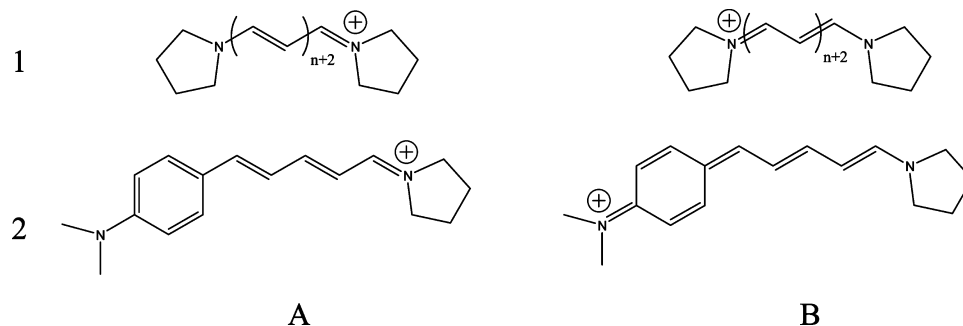


Figure 5. Lowest energy resonance structures of symmetric and unsymmetric cyanines. Without external field effects, the resonance structure B is of equal (1) and higher energy (2) than A. The symmetric 1 (Pyroliidino-*n*-SBP⁺) and the unsymmetric 2 (DMAPh-*n*-SBP⁺) are given as examples. For the nonsymmetric case 2, mesomeric coupling between structures A and B leads to a larger weight of structure A in the ground state and a surplus of positive charge at the molecular end as given in structure A. An external charge will influence the relative energy of these two structures and hence change their contribution in the wave function as well as in the charge distribution.

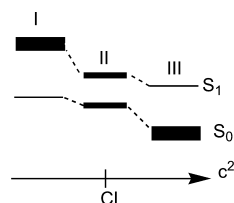


Figure 6. Schematic energy dependence of S_0 and S_1 states of unsymmetric cyanines and merocyanines on the energy difference of the resonance structures A and B, which determine the mixing coefficient c . For $c^2 = 0.5$, the two resonance structures have equal energy, and the energy gap ΔE_{01} is due to the interaction matrix element F and is smallest (CL, region II). In range I, structure A is more stable, and in range III, structure B is more stable. In both cases, the absorption energy increases. The transition from region I to II to III can occur by donor and acceptor substituents or by external charges (see below). The thickness of the lines indicates the relative contribution of resonance structure B in the wave function of the molecule.

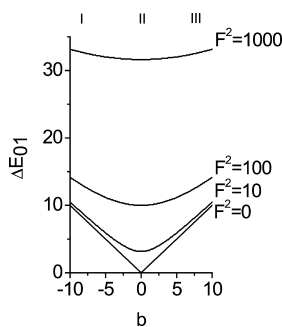


Figure 7. Model calculations for unsymmetric cyanines regarding the dependence of the absorption energy (in a.u.) on the coupling strength F and on the energy difference b (in a.u.) of the two main resonance structures according to eqs 3 and 4. F^2 values of 0, 10, 100, and 1000 are chosen as an example. $\Delta E_{DA} = b_A - b_B = b$ is the energy difference between the two resonance structures in Figure 5.

call it overpolarized case for unsymmetric compounds containing an aromatic ring like 2 in Figure 5 because the quinoid structure is normally the less stable one).

If a compound is close to CL ($c^2 = 0.5$), the effect of an external field will be smaller than for a compound with less evenly distributed positive charge (see also Figure 7). We can observe this effect for the methoxy donor (MOPh-2-SBP⁺, with a strongly asymmetric charge distribution, Figure 3, and MOPh-2-SBH⁺-bO). The MO-derivative shows an Opsin shift (2310 cm⁻¹) larger than the compound with the stronger donor (DMAPh-2-SBP⁺ and DMAPh-2-SBH⁺-bO, 1770 cm⁻¹), see Table 3, because MOPh-2-SBP⁺ is further away from the CL (less evenly distributed charge density). If a compound is

species	charge distribution	expected absorption shift
1.) charge distribution on the cationic chromophore including the effect of the counter ion		reference value
2.) additional "+" charge near the donor end ^{a)}		blue
3.) additional "+" charge near the acceptor end ^{b)}		red
4.) additional "+" charge in very close distance to the acceptor end or combined effect of "+" and "-" charges leads to "overpolarization" ^{c)}		little change with respect to case 3)

a) See the results of the experimental model compound study below. An equivalent change is induced by placing a negative charge near the acceptor end (e.g. the counterion in bR) or by decreasing the donor strength (in the compounds of our study).

b) an equivalent change is induced by placing a negative charge near the donor end or by decreasing the acceptor strength.

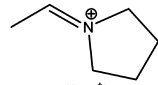
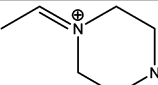
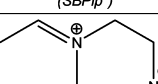
c) overpolarization: the majority of the positive charge in the ground state is situated at the end opposite to the acceptor group.

Figure 8. Influence of external positive or negative charges on the distribution of the positive charge along an unsymmetric cyanine (e.g., for DMAPh-2-SBP⁺). A more ground-state-extended charge distribution leads to an absorption red shift, and a more narrow one leads to a blue shift. In every case, the charge distribution in the excited state is opposite to that in the ground state.

at the CL and the charge is approximately evenly distributed, the longest-wavelength absorption will be present, and disturbance by a positive or negative charge at either end will lead to a blue shift. Applied to the compounds investigated here, a strong electrostatic field or an external charge which shifts the majority of the positive charge from the Schiff base to the donor end and thus reverts the original charge distribution, where the majority of the positive charge is located close to the Schiff base nitrogen, will cause overpolarization, that is, inversion of the charge distribution. Examples showing the above ideas are given in Figure 8. In cases where the switching from region I to III (Figure 6 and cases 3 and 4 in Figure 8) caused by overpolarization is symmetric, no shift is expected, whereas the strongest shift is expected for changes within regions I and II connected with a relative large slope in Figure 7 (cf. also Section B below).

The influence of an electrostatic field in region I is connected with a strong slope, that is, leads to a strong red shift and can yield an explanation for the Opsin shift of the chromophore in

TABLE 5: Calculated and Experimental Absorption Maxima for MOPh-1-R_A

acceptor end group R _A	λ _{abs} (nm)	
	calculation (INDO/S)	experimental (in ACN)
 (SBP ⁺)	418	374
 (SBPip ⁺)	419	376
 (SBPip ⁺⁺)	427	413

the bR environment. With respect to Figure 8, we explain the Opsin shift in the protein by three possibilities: (a) additional positive charge at the acceptor end of the chromophore, (b) additional negative charge at the donor end of the chromophore, or (c) increased distance of the counterion in the protein.

B. Investigation of Model Compounds with External Nonconjugated Charges. In order to study the polarization effect induced by external charges in more detail and to simulate an anisotropic electric field related to the field in the bR protein, we experimentally investigated a derivative of MOPh-1-SBP⁺ with an additional nonconjugated positive charge and performed detailed quantum-chemical calculations for comparison.

A chemical way of generating a nonconjugated positive charge near a dialkylamino group for a compound like DMAPH-2-SBP⁺ consists in the design of Schiff bases containing the piperazinium fragment (SBPip⁺) instead of the pyrrolidinium (SBP⁺) one. The second piperazinium nitrogen can be protonated in an acidic medium, and a model compound (acceptor end called SBPip⁺⁺) can be created with a surplus positive charge chemically attached close to the Schiff base nitrogen of the absorbing chromophore. Such molecules can serve as tests for investigating external-charge effects, both with experimental and quantum-chemical methods. Related experiments with nonconjugated charges close to the PRSB chromophore have been reported previously.^{17,46–52}

We could synthesize the doubly charged model compound MOPh-1-SBPip⁺⁺ and compare it to MOPh-1-SBPip⁺. We further have the comparison of experiment with quantum chemical calculations, and we can model the effect of the additional positive charge of the SBPip⁺⁺ compound on the charge distribution along the chromophore, the donor strength ΔE_{DA} , and the absorption maximum.

The results are summarized in Table 5.

As expected, the absorption energies, both experimental and calculated, do not differ significantly for the singly charged nonprotonated SBP⁺ and SBPip⁺ derivatives. This indicates that the influence of the slightly different N-alkyl groups near the Schiff base end can be neglected. The additional positive charge shifts the spectra only slightly to the red, consistently for experiment and calculation. The calculations underestimate the observed transition energy. For bR, an absorption shift of 44 nm from 550 nm at wild-type ebR (in E-coli expressed) to 594 nm at D85N in the dark adapted state (retinal in 13 cis form) was observed.⁵³ For the light adapted state (retinal in all trans) of D85N, a red shift of 33 nm compared to ebR was found.⁷ In the D85N, the deprotonated negative aspartic acid (D) in the

TABLE 6: Percentage of Charge Located on Donor and Acceptor Moieties, Together with Transition Energies, Donor–Acceptor Strength ΔE_{DA} , and Charge-Distribution Enhancement as Determined from ZINDO/S Calculations

molecule	ΔE_{DA} (eV)	Q_D^a	Q_A^b	ΔE_{01} (eV)	Q_{ED}^c
For $n = 1$ Compounds					
HPh-1-SBP ⁺	-4.093	17	83	3.206	
MPh-1-SBP ⁺	-3.770	18	82	3.057	
HOPh-1-SBP ⁺	-3.554	19	81	2.996	
MOPh-1-SBP ⁺	-3.444	21	79	2.965	
DMAPH-1-SBP ⁺	-2.714	28	72	2.691	
HPh-1-SBPip ⁺	-4.059	17	83	3.200	
MPh-1-SBPip ⁺	-3.736	18	82	3.051	
HOPh-1-SBPip ⁺	-3.520	20	80	2.991	
MOPh-1-SBPip ⁺	-3.410	21	79	2.959	
DMAPH-1-SBPip ⁺	-2.680	28	72	2.685	
HPh-1-SBPip ⁺²	-0.163	36	64	3.068	19
MPh-1-SBPip ⁺²	0.160	41	59	2.965	23
HOPh-1-SBPip ⁺²	0.376	45	55	2.924	26
MOPh-1-SBPip ⁺²	0.486	48	52	2.905	27
DMAPH-1-SBPip ⁺²	1.216	62	38	2.805	34
For $n = 2$ Compounds					
HPh-2-SBP ⁺	-4.093	12	88	2.762	
MPh-2-SBP ⁺	-3.770	13	87	2.653	
HOPh-2-SBP ⁺	-3.554	14	86	2.616	
MOPh-2-SBP ⁺	-3.444	15	85	2.591	
DMAPH-2-SBP ⁺	-2.714	23	77	2.367	
HPh-2-SBPip ⁺	-4.059	12	88	2.756	
MPh-2-SBPip ⁺	-3.736	13	87	2.648	
HOPh-2-SBPip ⁺	-3.520	15	85	2.611	
MOPh-2-SBPip ⁺	-3.410	16	84	2.586	
DMAPH-2-SBPip ⁺	-2.680	23	77	2.361	
HPh-2-SBPip ⁺²	-0.163	33	67	2.687	21
MPh-2-SBPip ⁺²	0.160	38	62	2.630	25
HOPh-2-SBPip ⁺²	0.376	42	58	2.610	28
MOPh-2-SBPip ⁺²	0.486	46	54	2.608	31
DMAPH-2-SBPip ⁺²	1.216	60	40	2.586	37

^a $Q_D = q_D/(q_D + q_A)$ in percent. ^b $Q_A = 100 - Q_D$ in percent. ^c Charge-distribution enhancement: $Q_{ED} = Q_D(R_DPh-n-SBPip^{+2}) - Q_D(R_DPh-n-SBP^+)$.

counterion is substituted by the neutral but hydrophilic asparagine (N). This fits quite well with the observed 37 nm shift from SBPip⁺ to SBPip⁺² in ACN, see Table 5. In the dark-adapted form of R82A and R82Q (positive arginine replaced by a neutral residue), the absorption is blue-shifted to 547 nm. Later (1999), it was found by X-ray crystallography³ that these residues, D85, R82, and D212, together with some water molecules, belong to a distributed counterion connected by hydrogen bonds where the negative D85⁻ exhibits the smallest distance to the protonated Schiff base. In the triple mutant where all three charged residues of the counterion are replaced by neutral ones, the retinal chromophore can bind if some millimolar salt is added.⁷ The color depends on the anion radius (549, 563, 573, and 580 nm for F⁻, Cl⁻, Br⁻, and I⁻, respectively), indicating that the smaller anions may come closer to the Schiff base generating a bigger blue shift.

The experimental results for MOPh-1-R_A were supplemented with the full set of calculations for a range of donors and both series $n = 1$ and $n = 2$. In this way, charge distribution and absorption energy can be contrasted.

These results are summarized in Table 6.

As can be seen, the somewhat unsymmetric charge distribution of the singly charged cations is strongly polarized by adding an additional positive charge. The corresponding absorption energies can be determined by quantum-chemical treatment and compared to experiment (see Figure 3 and Table 4). Two cases

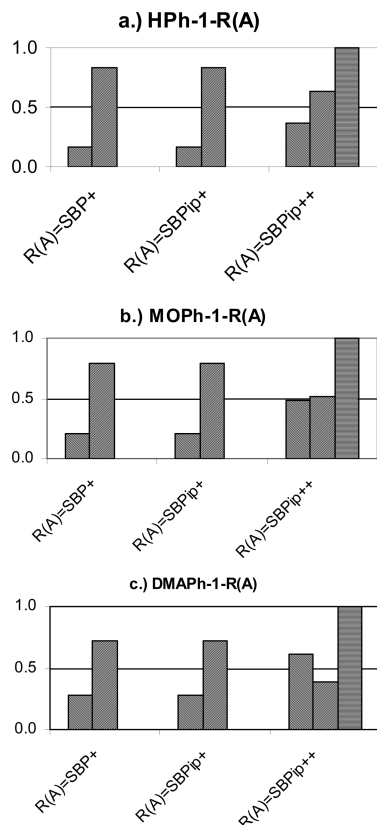


Figure 9. Fraction of the positive charge Q_D (left bar) located on the donor unit and fraction of the positive charge Q_A (right bar) located on the acceptor unit of R_D Ph-1- R_A compounds with a single positive charge (SBP^+ and $SBPip^+$ compounds) and with an additional nonconjugated charge ($SBPip^{++}$, outermost bar at the right). The cases $R_D = H, MO,$ and DMA are shown.

of overpolarization can be observed and are shown in Figures 9 and 10. For reference, SBP^+ and $SBPip^+$ derivatives are compared, and their charge distribution differs very little, as expected.

As can be seen in these figures, the field of the additional positive nonconjugated charge near the Schiff base nitrogen polarizes the distribution of the positive charge on the molecule in such a way that the positive charge moves away from the Schiff base nitrogen toward the donor, as qualitatively outlined in Figure 8. For donors $R_D = H$ and MO , the external charge modifies the original charge distribution but does not revert it. In the case of the dimethylamino compounds ($R_D = DMA$), a charge reversal is observed; that is, a charge distribution results where a surplus of charge is located on the donor unit. This corresponds to situation 4 in Figure 8, that is, to the valence structure B being more stable than structure A (Figure 5). In terms of the resonance model, we are in the region III (Figure 6), and the ground-state wave function carries a larger weight of B ($c^2 > 0.5$); hence, the unequal superposition by resonance of the two valence-bond structures leads to a surplus of positive charge near the aminophenyl group, resulting from structure B (Figure 5). We call region III in Figure 6 the overpolarized region, because the field reverts the original charge distribution.

If a field causes overpolarization from region I (polarization) to III (overpolarization), the CL (region II) has to be crossed. Starting from the CL, polarization toward the region I and overpolarization toward the region III both lead to a blue shift (Figure 8); hence, if the polarization/overpolarization is symmetric with respect to CL, no shift will be observed. There can even be a blue shift induced by the charge, if overpolarization

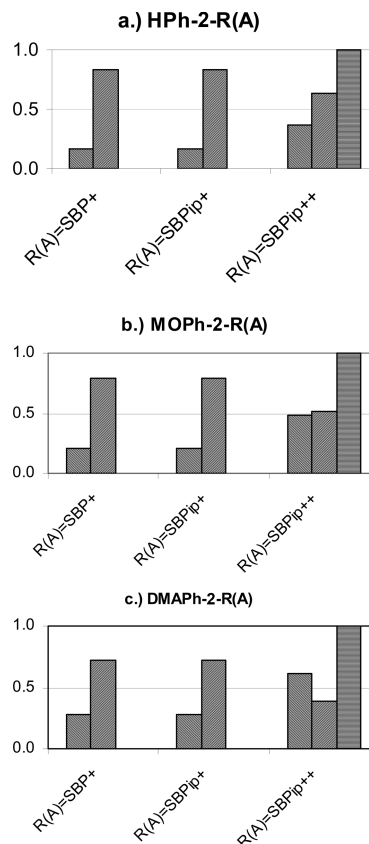


Figure 10. Fraction of the positive charge Q_D (left bar) located on the donor unit and fraction of the positive charge Q_A (right bar) located on the acceptor unit of R_D Ph-2- R_A compounds with a single positive charge (SBP^+ and $SBPip^+$ compounds) and with an additional nonconjugated charge ($SBPip^{++}$, outermost bar at the right). The cases $R_D = H, MO,$ and DMA are shown.

by the nonconjugated charge is stronger than polarization (without the additional field) although the compound is originally in region I.

The calculations summarized in Table 6 in fact show this to be the case. This is visualized in Figure 11, which shows that the change of the absorption energy E_{01} is different for every compound and can correspond to either a red shift ($R_D = H$), a blue shift ($R_D = DMA$), or nearly constant energy ($R_D = MO$). Hence, $MOPh-1-SBPip^+$ and $MOPh-2-SBPip^+$ in the gas phase are nearly symmetric cases with respect to CL. We notice that the charge distribution remains, nevertheless, biased toward the Schiff base nitrogen. The reason for this is that the phenyl groups possess aromatic character, and hence, the resonance structure A (with the aromatic phenyl ring) has a weight larger (>50%) than expected from the simplified eqs 1 and 2. This has been outlined in detail previously for the case of stilbenes, where the weight of the aromatic structures is even more emphasized.^{25,54}

The ΔE_{DA} values (see calculational part) derived from the energies of HOMO(D) and LUMO(A) in Table 4 are related to the energy difference b between resonance structures A and B, and it can be seen that the external charge increases ΔE_{DA} toward less negative or even positive values (Table 6), that is, toward CL (for H and MO) and beyond (region III in Figure 6 for DMA). The absorption energies (Table 6) behave according to eq 4 and Figure 7: red shift for the weaker donors (range I), blue shift for the strong donors (range III), and some intermediate cases with no shift (range II near CL).

This behavior is emphasized in Figure 11, which compares the two series $n = 1$ and 2. As can be seen, for $n = 2$ and the

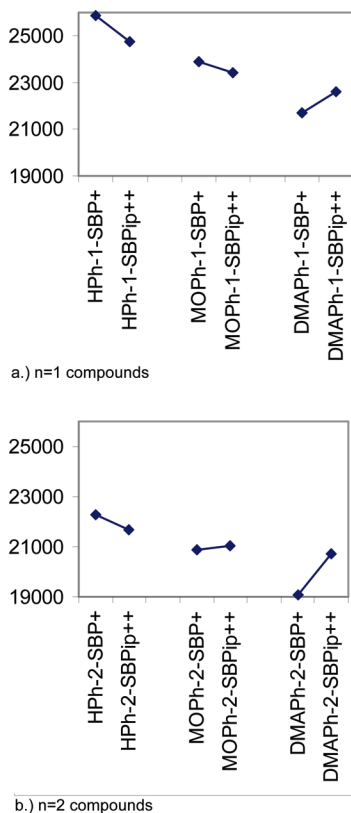


Figure 11. Calculated shift of the absorption energy with introduction of an external positive charge near the Schiff base nitrogen as a function of the donor strength (H, MO, and DMA compounds) and the chain length ($n = 1, 2$).

strong donor DMA, the blue shift with introduction of the charge and due to overpolarization is stronger for the $n = 2$ series. This indicates that for the $n = 2$ series, smaller electric fields are necessary to reach the CL or cross it to the overpolarized region.

Table 6 also includes the charge distribution enhancement Q_{ED} , which mirrors the larger sensitivity to the additional charge of the $n = 2$ series and of the compounds with intermediate donor strength (MOPh).

For the experimental results of the chromophore–bO complexes, the shift is invariably to the red, that is, corresponding to range I. We can thus conclude that the electrostatic field present in Bacterioopsin is much smaller than that in our model compound with a surplus positive charge in close proximity to the positively charged Schiff base nitrogen. Model calculations of the chromophores with various charges in the surrounding should be able to reproduce the Opsin shift observed (Table 3). This work is in progress.

Summary

The change of the absorption energy and the charge distribution in the compounds investigated both in solution and as chromophore–Bacterioopsin complexes have been shown to be related to the difference of the donor and acceptor strength of the substituents, as well as to the external electrostatic field created by an external charge. These effects can be simulated by quantum-chemical-model calculations, giving evidence that in some compounds, the role of the main resonance structure is reversed for the ground and excited states (overpolarized case). In this context, the concept of the CL is of importance and allows us to describe the changes in absorption energy by using

a simple 2×2 interaction model (and neglecting further weaker interactions which are also present).

The observed Opsin shifts for the chromophore–protein complexes can be correlated with the donor–acceptor strength and yield quantitative information regarding the placement of the chromophores with respect to the CL.

The charge distribution of the chromophore is also linked to the CL, and in the overpolarized case, the majority of the positive charge is far away from the Schiff base nitrogen. The sensitivity of this effect depends on the donor property of the substituent and on the chain length n , being stronger for longer chains. The new approach using variable donor–acceptor strength of protein-embedded model chromophores can also yield new insight into the mechanism of the Opsin shift.

Acknowledgment. We thank the International Bureaux of the Ministry of Research and Technology (WTZ-Projekt UKR 02/004) for support of this work through a travel grant to J.B. The authors are grateful for the support of M. Heyn and J. Heberle, Free University of Berlin.

Supporting Information Available: This material is available free of charge via the Internet at <http://pubs.acs.org>.

References and Notes

- Palczewski, K.; Kumasaka, T.; Hori, T.; Behnke, C. A.; Motoshima, H.; Fox, B. A.; Le Trong, I.; Teller, D. C.; Okada, T.; Stenkamp, R. E.; Yamamoto, M.; Miyano, M. *Science* **2000**, *289*, 739.
- Okada, T.; Fujiyoshi, Y.; Silow, M.; Navarro, J.; Landau, E. M.; Shichida, Y. *Proc. Natl. Acad. Sci. U.S.A.* **2002**, *99*, 5982.
- Luecke, H.; Schobert, B.; Richter, H.-T.; Cartailler, J.-P.; Lanyi, J. K. *J. Mol. Biol.* **1999**, *291*, 899.
- Sekharan, S.; Sugihara, M.; Buss, V. *Angew. Chem., Int. Ed.* **2007**, *46*, 269.
- Fujimoto, K.; Hayashi, S.; Hasegawa, J.; Nakatsuji, H. *J. Chem. Theory Comput.* **2007**, *3*, 605.
- Kleinschmidt, J.; Harosi, F. *Proc. Natl. Acad. Sci. U.S.A.* **1992**, *89*, 9181.
- Marti, T.; Rösselet, S.; Otto, H.; Heyn, M. P.; Khorana, H. G. *J. Biol. Chem.* **1991**, *266*, 18674.
- Marti, T.; Otto, H.; Rösselet, S.; Heyn, M. P.; Khorana, H. G. *J. Biol. Chem.* **1992**, *267*, 16922.
- Hoffmann, M.; Wanko, M.; Strodel, P.; König, P. H.; Frauenheim, T.; Schulten, K.; Tajkhorshid, E.; Elstner, M. *J. Am. Chem. Soc.* **2006**, *128*, 10808.
- See for instance pdb files 1c3w and 2at9.
- Aton, B.; Doukas, A.; Callender, R.; Becher, B.; Ebre, T. *Biochemistry* **1977**, *16*, 2995.
- Balogh-Nair, V.; Carrier, J. D.; Honig, B.; Kamat, V.; Motto, M. G.; Nakanishi, K.; Sen, R.; Sheves, M.; Arnaboldi Tanis, M.; Tsujimoto, K. *Photochem. Photobiol.* **1981**, *33*, 483.
- Nakanishi, K.; Balogh-Nair, V.; Arnaboldi, M.; Tsujimoto, K.; Honig, B. *J. Am. Chem. Soc.* **1980**, *102*, 7945.
- Derguini, F.; Caldwell, C. G.; Motto, M. G.; Balogh-Nair, V.; Nakanishi, K. *J. Am. Chem. Soc.* **1983**, *105*, 646.
- Lugtenburg, J.; Muradin-Szweykowska, M.; Heeremans, C.; Pardo, J. A.; Harbison, G. S.; Herzfeld, J.; Griffin, R. G.; Smith, S. O.; Mathies, R. A. *J. Am. Chem. Soc.* **1986**, *108*, 3104–5.
- Sheves, M.; Albeck, A.; Baasov, T.; Friedman, N.; Ottolenghi, M. *Retinal Proteins*; VNU Science Press, 1987; pp 201–216.
- Baasov, T.; Sheves, M. *J. Am. Chem. Soc.* **1987**, *109*, 1594.
- Andersen, L. H.; Nielsen, I. B.; Kristensen, M. B.; El Ghazaly, M. O.; Haacke, S.; Nielsen, M. B.; Petersen, M. A. *J. Am. Chem. Soc.* **2005**, *127*, 12347.
- Lin, S. W.; Kochendoerfer, G. G.; Carroll, K. S.; Wang, D.; Mathies, R. A.; Sakmar, T. P. *J. Biol. Chem.* **1998**, *273*, 24583.
- Kochendoerfer, G. G.; Lin, S. W.; Sakmar, T. P.; Mathies, R. A. *Trends Biochem. Sci.* **1999**, *24*, 300.
- Sun, H.; Macke, J. P.; Nathans, J. *Proc. Natl. Acad. Sci. U.S.A.* **1997**, *94*, 8860.
- Stenkamp, R. E.; Filipek, S.; Driessen, C. A. G. G.; Teller, D. C.; Palczewski, K. *Biochim. Biophys. Acta* **2002**, *1565*, 168.
- Sun, H.; Macke, J. P.; Nathans, J. *Proc. Natl. Acad. Sci. U.S.A.* **1997**, *94*, 8860.
- van den Berg, R.; Du-Jeon-Jang; Bitting, H. C.; El-Sayed, M. A. *Biophys. J.* **1990**, *58*, 135.

- (25) Dekhtyar, M.; Rettig, W. *J. Phys. Chem. A* **2007**, 2035.
- (26) Friedli, A. C.; Yang, E.; Marder, S. R. *Tetrahedron* **1997**, 53 (No 8), 2717–2730.
- (27) Bricks, J. In preparation.
- (28) Peak Fit is a registered trademark of Systat Software Inc., www.systat.com.
- (29) Oesterhelt, D. *Methods Enzymol.* **1982**, 88, 10–17.
- (30) Frisch, M. J.; Trucks, G. W.; Schlegel, H. B.; Scuseria, G. E.; Robb, M. A.; Cheeseman, J. R.; Montgomery, Jr., J. A.; Vreven, T.; Kudin, K. N.; Burant, J. C.; Millam, J. M.; Iyengar, S. S.; Tomasi, J.; Barone, V.; Mennucci, B.; Cossi, M.; Scalmani, G.; Rega, N.; Petersson, G. A.; Nakatsuji, H.; Hada, M.; Ehara, M.; Toyota, K.; Fukuda, R.; Hasegawa, J.; Ishida, M.; Nakajima, T.; Honda, Y.; Kitao, O.; Nakai, H.; Klene, M.; Li, X.; Knox, J. E.; Hratchian, H. P.; Cross, J. B.; Bakken, V.; Adamo, C.; Jaramillo, J.; Gomperts, R.; Stratmann, R. E.; Yazyev, O.; Austin, A. J.; Cammi, R.; Pomelli, C.; Ochterski, J. W.; Ayala, P. Y.; Morokuma, K.; Voth, G. A.; Salvador, P.; Dannenberg, J. J.; Zakrzewski, V. G.; Dapprich, S.; Daniels, A. D.; Strain, M. C.; Farkas, O.; Malick, D. K.; Rabuck, A. D.; Raghavachari, K.; Foresman, J. B.; Ortiz, J. V.; Cui, Q.; Baboul, A. G.; Clifford, S.; Cioslowski, J.; Stefanov, B. B.; Liu, G.; Liashenko, A.; Piskorz, P.; Komaromi, I.; Martin, R. L.; Fox, D. J.; Keith, T.; Al-Laham, M. A.; Peng, C. Y.; Nanayakkara, A.; Challacombe, M.; Gill, P. M. W.; Johnson, B.; Chen, W.; Wong, M. W.; Gonzalez, C.; Pople, J. A. *Gaussian 03*, Revision D.01; Gaussian, Inc.: Wallingford CT, 2004.
- (31) Solvatochromy is also nearly absent for closely related ionic stilbazolium derivatives, see Ephardt, H.; Fromherz, P. *J. Phys. Chem.* **1991**, 95, 6792.
- (32) Dähne, S.; Hoffmann, K. In *Progress in Physical Organic Chemistry*; Taft, W., Ed.; J. Wiley & Sons, Inc., 1990; Vol. 18, pp 1–64.
- (33) Lippert, E. *Ber. Bunsenges. Phys. Chem.* **1957**, 61, 962.
- (34) Th. Förster, Z. *Elektrochem. Angew. Physik. Chem.* **1939**, 45, 571.
- (35) Platt, J. R. *J. Chem. Phys.* **1956**, 25, 80.
- (36) Dähne, S.; Moldenhauer, F. In *Progress in Physical Organic Chemistry*; Taft, W., Ed.; John Wiley & Sons, Inc., 1995; Vol. 15, pp 1–130.
- (37) Dähne, S.; Leupold, D. *Ber. Bunsenges. Phys. Chem.* **1966**, 70, 618.
- (38) Andersen, L. H.; Nielsen, I. B.; Kristensen, M. B.; El-Ghazaly, M. O. A.; Haacke, S.; Nielsen, M. B.; Petersen, M. A. *J. Am. Chem. Soc.* **2005**, 127, 12347.
- (39) Freedman, K. A.; Becker, R. S. *J. Am. Chem. Soc.* **1986**, 108, 1245.
- (40) Lanyi, J. K. *Nature* **1995**, 375, 461.
- (41) Dähne, S.; Radeaglia, R. *Tetrahedron* **1971**, 27, 3673.
- (42) Brooker, L. G. S. *Rev. mod. Physics* **1942**, 14, 275.
- (43) Tyutyulkov, N.; Fabian, J.; Mehlhorn, A.; Fietz, F.; Tadjer, A. *Polymethine Dyes. Structure and Properties*; St. Kliment Ohridski University Press: Sofia/Bulgaria, 1991.
- (44) Dyadyusha, G. G.; Kachkovskii, A. D. *Ukr. Khim. Zh.* **1975**, 41, 1176.
- (45) (a) Dyadyusha, G. G.; Kachkovskii, A. D. *Theor. Eksp. Khim.* **1979**, 15, 152. (b) Dyadyusha, G. G.; Kachkovskii, A. D. *Theor. Eksp. Khim.* **1981**, 17, 393.
- (46) Sheves, M.; Nakanishi, K. *J. Am. Chem. Soc.* **1983**, 105, 4033.
- (47) Baasov, T.; Sheves, M. *J. Am. Chem. Soc.* **1985**, 107, 7524.
- (48) Sheves, M.; Friedman, N. *Angew. Chem., Int. Ed. Engl.* **1986**, 25, 284.
- (49) Baasov, T.; Sheves, M. *Biochemistry* **1986**, 25, 5249.
- (50) Sheves, M.; Albeck, A.; Baasov, T.; Friedman, N.; Ottolenghi, M. *Retinal Proteins*; VNU Science Press, 1987; pp 201–216.
- (51) Baasov, T.; Friedman, N.; Sheves, M. *Biochem.* **1987**, 26, 3210.
- (52) Albeck, A.; Livnah, N.; Gottlieb, H.; Sheves, M. *J. Am. Chem. Soc.* **1992**, 114, 2400.
- (53) Otto, H.; Marti, T.; Holz, M.; Mogi, T.; Stern, L. J.; Engel, F.; Korana, H. G.; Heyn, M. P. *Proc. Natl. Acad. Sci. U.S.A.* **1990**, 87, 1018.
- (54) Rettig, W.; Dekhtyar, M. *Chem. Phys.* **2003**, 293, 75.

JP904132F